Synthesis, morphology and electrical property characteristics of MXene based titanium carbide ($Ti_3C_2T_x$) coating on non-woven cotton paper

R. Jothiramalingam[a,*], T. Radhika[b], N. P. Kavitha[c], H. Al-Lohedan[a], D. M. Aldhayan, M. Karnan[d]

[a] *Department of Chemistry, College of Science, King Saud University, P.O. Box.2455, Riyadh 11451, Saudi Arabia*

[b]*Center for Materials for Electronics Technology [C-MET], M.G. Kavu Thrissur, Kerala-680581, India.*

[c]*Department of Chemical Engineering, Sri Venkateshwara College of Engineering, Sriperumbudur, Kancheepuram, 602117, India*

[d]*Grassland and Forage Division, National Institute of Animal Science, Rural Development Administration, Chungcheongnam-do, Cheonan 31000, South Korea*

In the present study, $Ti_3C_2T_x$ type MXene was prepared by selective etching of Al from Ti_3AlC_2 with mesh size of 200. The powder form of raw material was used to fabricate $Ti_3C_2T_x$ by in-situ HF etching method. The MXene is further coated on non-woven paper by simply dip coating method. The detailed structural, morphology and elemental content study of as prepared $Ti_3C_2T_x$ MXene have demonstrated. The MXene (Ti_3AlC_2) powders show compact, layered morphology as expected for bulk layered ternary carbide. The detailed elemental analysis has carried out for Titanium carbide based MXene coated and uncoated woven paper. The lower conducting property obtained for paper coating due less amount of coating in the surface of paper instead of coating on glass substrate. The electrical property characterization of MXene coated non-woven paper and glass substrate have also been studied. Hence, the conductive coating of MXene-in water formulation achieved through simple dip coating methods is promising for low cost sensor, wearable shielding device fabrication towards renewable energy and healthcare applications.

(Received June 1, 2023; Accepted January 2, 2024)

Keywords: $Ti_3C_2T_x$, MXene, Non-woven, Cotton, Dip coating, Strain sensor

1. Introduction

Simple stretchable ready to use pressure/strain sensors are more attractable due to its unlimited applications in robots with soft bodies, because of its potential applications in anthropological monitoring, synthetic electronic skin, machine–man interactions, speech therapy systems, and so forth [1]. These properties are not sufficient for highly sensitive applications that would have the gauge factor (GF) of above 100 and above 50% (Broad sense) necessary but it is still a big challenge to get this dual one [2]. Many researchers have done research works to overcome the challenges to meet the real-time application requirement and observed remarkable findings. Ag nanowires with polydopamine fabrication by dip-coating yield a significant flexible cotton-based strain sensor with a low GF. High GF of 5000 was attained in strain sensors of highly sensitive metal-based thin film with the eminent ability of micro-crack structure but with the constraint of a 1% sensing range. The materials with microcrack structure give good appeal the strain sensor-related researchers to give a drive to enhance the GF and sensing range. With these conclusions, some fibrous materials with Knudsen porous structure fabrics like graphene/polyamide interlocking fabrics, graphene/polyester fabrics, graphene/ poly (3, 4-ethylene dioxythiophene) polystyrene sulfonate (PEDOT: PSS)/wool-nylon composite fabrics and so forth[3].

* Corresponding author: profjothiram@gmail.com
https://doi.org/10.15251/DJNB.2024.191.15

Carbon-based nanocomposites and it's derived various structural materials like wires, tubes, etc. are considered to be good candidates for the fabrication of EPCPs base sensors. Even though, these are having good admirable qualities, high affinity towards polymers and reasonable dispersive nature are the concerns related to these materials. We need to alleviate these issues with an alternative such that transition metal of three-dimensional materials like Ti_3C_2Tx [4]. The fabricated wearable Ti_3C_2Tx MXene strain sensor modules showed a good response of sensitivity and integrating with ML chip, fabrication of an edge sensor was developed and exhibited good animation response without any computing platforms [5]. Redondo & Pumera, 2021, synthesized Mxene materials with high elasticity of 36507 under a yield stress of 206 Pa and viscoelasticity behavior proved to be a remarkable candidate for 3D printing. These properties are also applicable to wearable sensors and biomedical applications [6-11]. The layered structure Mxenes with high gas adsorption abundant surface area towards single selective molecules from gas consortia, superior sensitivity by same as metallic conductivity, high gas-to-noise ratio, and frequent electrical response comes into picture to enforce the researchers to fabricate these highly comfortable and sensitive materials for pollutant detection wearable strain sensors [12-13].

The aim of the present research work is to fabricate low-cost Ti_3C_2Tx MXene-coated non-woven paper and coating on membrane or glass substrate for improved conductive properties and wearable sensor applications. Detailed structural and morphology characterization have been demonstrated for coated and uncoated non-woven paper materials.

2. Experimental

The $Ti_3C_2T_x$ MXene was produced through selective Al etching from Ti_3AlC_2 (Forsman, 98%), and mesh size was 200, and powder form material used for in-situ HF etching technique. In a typical process, LiF (Alfa Aesar, 98.5 %) was mixed with HCl solution (9 molar) in 100 mL polytetrafluoroethylene bottle. To completely dissolve LiF, the liquid was agitated for 5 minutes. To this, Ti_3AlC_2 (Forsman, 200 size mesh, 98% purity) was added slowly maintaining 45 ^oC temperature. This mixture was stirred for 24 h. The resulting solution was centrifuged to separate the supernatant after being diluted with d.H2O. The washing with d.H_2O has been carried out repeatedly until the pH of the supernatant reached greater than or equal to 6. The sediment was diluted in 100 mL and delamination of $Ti_3C_2T_x$ clay formed was done by sonication for 10 minutes. The mixture was once more centrifuged, and the delaminated $Ti_3C_2T_x$ MXene nanosheet supernatant was collected for further research.

The chemical reaction is,

$$3\ HCl + 3\ LiF \longrightarrow 3HF + 3\ LiCl \quad (1)$$

After the dissolving LiF, Ti_3AlC_2 was added into the solution at a temperature of 45 °C. Stirring continued for 24 hrs. The etching reaction equations are as follows:

$$M_{n+1}Al\ X_n + 3HF \longrightarrow M_{n+1}X_n + Al\ F_3 + 3/2\ H_2 \quad (2)$$

$$M_{n+1}X_n + 2HF \longrightarrow M_{n+1}X_nF_2 + H_2 \quad (3)$$

$$M_{n+1}X_n + 2H_2O \longrightarrow M_{n+1}X_n(OH) + H_2 \quad (4)$$

3. Material characterization

On advanced diffractometer, RAD III from Rigaku, Japan, using Cu Kα radiation (λ=1.54 Å), the crystal structure of the materials and coated surface were studied. The patterns between 5° and 70° were captured at 10/min scan rate. Materials were analyzed using SEM ("Scanning Electron Microscopy") and EDAX ("Energy-Dispersive Spectroscopy") on a "Carl Zeiss UK EVO18-9 SEM" with an EDS scheme. On ECOPIA HALL EFFECT MEASUREMENT

SYSTEM, electrical conductivity evaluations have been made using the 4-probe technique at normal temperature ("HMS-3000 VER 3.51.5").

The synthesis process of $Ti_3C_2T_x$ is shown in the form of flow chart.

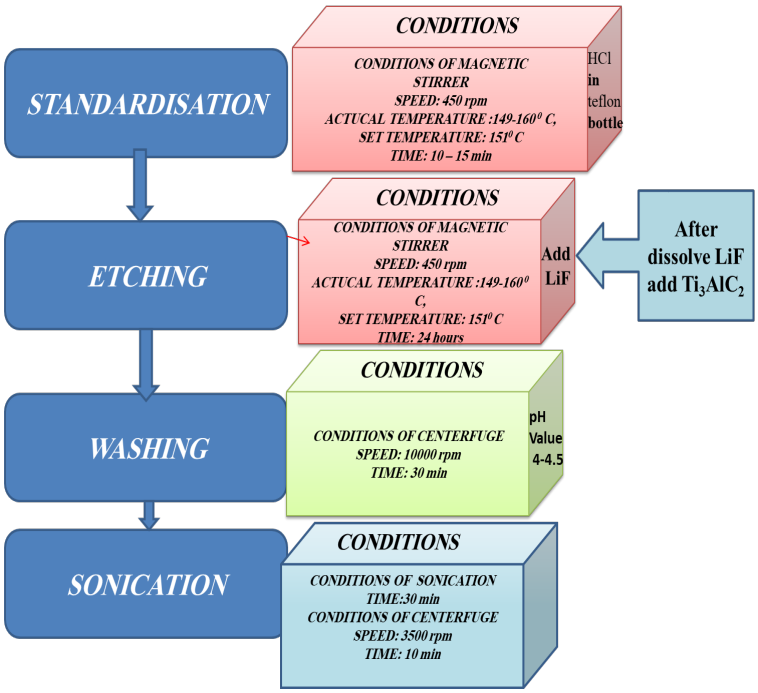

Scheme 1. Fabrication process of Titanium carbide based MXene from Ti_2AlC_2.

4. Results and discussion

4.1. Powder X-ray diffraction (XRD) analysis

The effective synthesis of Ti_3C_2Tx MXene from Ti_3AlC_2 MAX phases must be demonstrated using the powder X-ray diffraction technique. It is evident from the Ti_3C_2Tx pattern that a few of the distinctive diffraction peaks of Ti_3AlC_2 have vanished or diminished in intensity and a few new peaks have emerged (Figure 1). It demonstrates that under the investigated conditions, Ti_3AlC_2 is etched to produce Ti_3AlC_2 MXene, which contains Al atoms. The Al layer removal from Ti_3AlC_2 resulted in a loss of all Ti_3AlC_2-associated peaks and the shift of (002) and (004) peaks toward lower values, from 2θ=9.57◦ and 19.19◦ to 2θ = 8.86◦ and 18.04◦ resp. Generally, shift and broadening of (002) peak denoted that $Ti_3AlC_2$was successfully formed [14-16]. The XRD pattern of MX16 is depicted in Figure 4.5(e). In this pattern, the (002) peak shifts to a lower 2θangle (6.69°) that shows Ti_3C_2 formation. The (006) peak of $Ti_3C_2T_x$ at 28.91° indicates the presence of $Ti_3C_2(OH)_2$. The reduction of the (104) peak demonstrates that Al has been completely etched from the MAX phase to generate delaminated Ti_3CxTx.

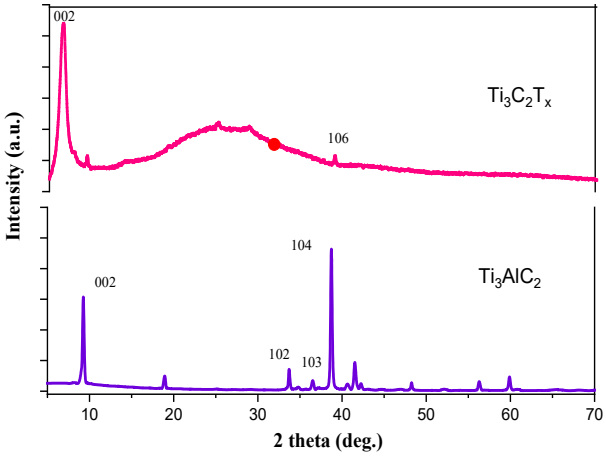

Fig. 1. XRD pattern of MXene, P0, P1, P2, P3, P4.

4.2 Morphology analysis

The morphology of the Ti_3AlC_2 and $Ti_3C_2T_x$ were observed by SEM. Elemental composition was analyzed by EDAX ("Energy dispersive electron X-ray").

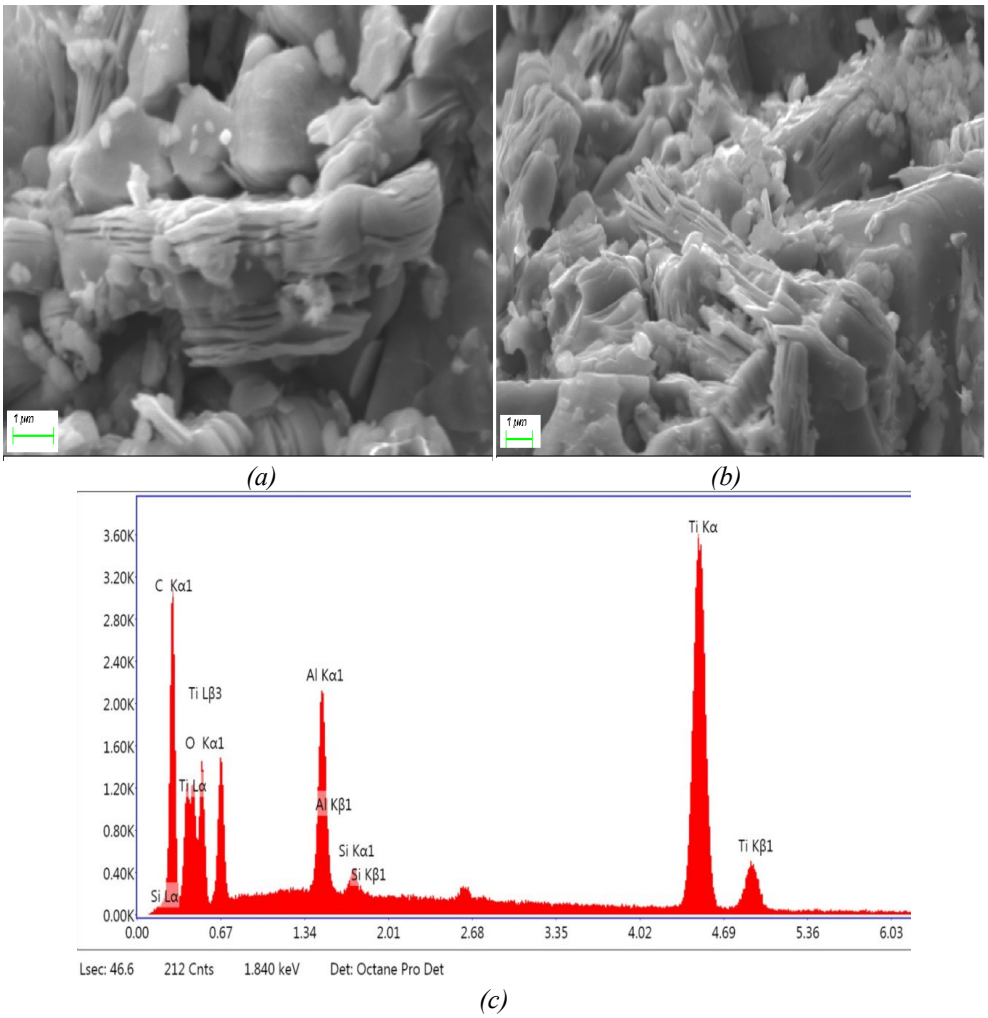

Fig. 2. (a and b) Scanning electron micrographs $Ti_3C_2T_x$ and (c) EDAX of $Ti_3C_2T_x$ (P1)

The SEM images and EDAX of Ti_3AlC_2 are depicted in Figure 2 (a) and (b). The morphology of Ti_3AlC_2 reveals that Ti_3AlC_2 grains are plate-like and it is densely stacked. As expected for bulk layered ternary carbide, the morphology of Ti_3AlC_2 particles is compact and layered. During synthesis of Ti_3AlC_2, Si is added as a catalyst to speed up the reaction. In final stage of synthesis, most of the Si replaced Al due to high temperature. Ti_3AlC_2 bulk material was synthesized by hot pressing with elemental powder mixture of Al, Ti, Si, and active carbon having molar ratios 2.0Ti/1.1Al/1.0C, 0.1mol Al replaced by Si and 0.2mol Al replaced by Si. The EDAX of Ti_3AlC_2 shows the major elements as Al, Ti, and C. The shape of Ti_3AlC_2 powders (Figure 2a) is compact and layered, as would be predicted for bulk-layered ternary carbide. The layers are separated and parallel to one another after etching, as depicted in Figure. Such morphological changes are consistent with those reported in the literature, indicating that Ti_3AlC_2 has selectively removed Al layers. The etching of Al was verified using EDS on both Ti_3AlC_2 and Ti3C2Tx powders. The $Ti_3C_2T_x$ included very little Al component, according to the EDS investigation, and the Al concentration had drastically dropped.

Ti_3AlC_2 powders show compact, layered morphology (Figures 2a) as expected for bulk layered ternary carbide. After etching, the layers are separated and parallel to each other, as shown in Figure. 4a and 4b. Such morphological transformations are similar to those observed in the literature, which indicates the selective removal of Al layers in Ti_3AlC_2. EDS was carried out on both Ti_3AlC_2 and $Ti_3C_2T_x$ powders to confirm the etching of Al. From the EDS analysis, the content of Al significantly decreased and a very small amount of Al component was found in the $Ti_3C_2T_x$ (Fig. 4c).

4.3. Dip coating of Non-woven cotton paper fabrication

The colloidal solution of delaminated $Ti_3C_2T_x$ in water obtained by etching and further washing process was used for coating on non-woven paper. The methods adopted for coating is dip coating process. Prior to dip coating, the washed non-woven paper was dipped into the $Ti_3C_2T_x$ in water formulation, dried in laboratory oven for 2 hours and the process was repeated for 3-4 times. Figure 3 shows the dip coating as properad $Ti_3C_2T_x$ at various time intervals and it designated as P0, P1, P2, P3 and P4. Figure 4 shows FE-SEM images of coated and uncoated MXene non-woven paper materials

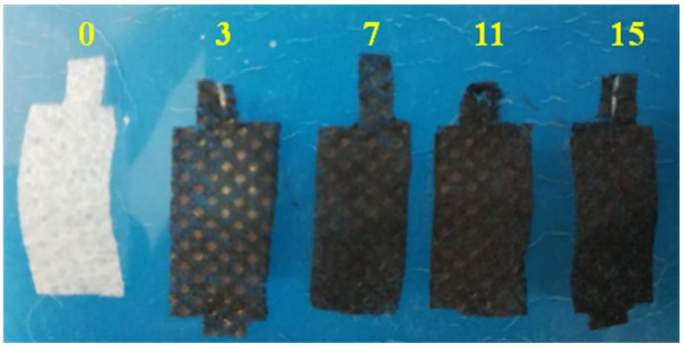

Fig. 3. Dip coating method prepared non-woven paper materials at different coating time (P0-P4).

Figure 4 shows the SEM images of higher magnification (200 micrometer) to lower magnification (10 micrometer) scale of coated uncoated non-woven paper. In comparison to P0, P1 to P4 coating is well coated with aggregation of Titanium carbide ($Ti_3C_2T_x$) particle obtained on fibrous morphology of base material and it is well coated like reported methods [17-20]. Improved deposition obtained with respect to deposition time or dip coating duration. Figure 5, further demonstrate the elemental content analysis of coated ($Ti_3C_2T_x$). At P0 condition only 100% carbide content recorded at the initial time and after dip coating process starts on non-oven paper cloth material enhance the more titanium metal content deposition and decreased carbon content observed for the coated materials.

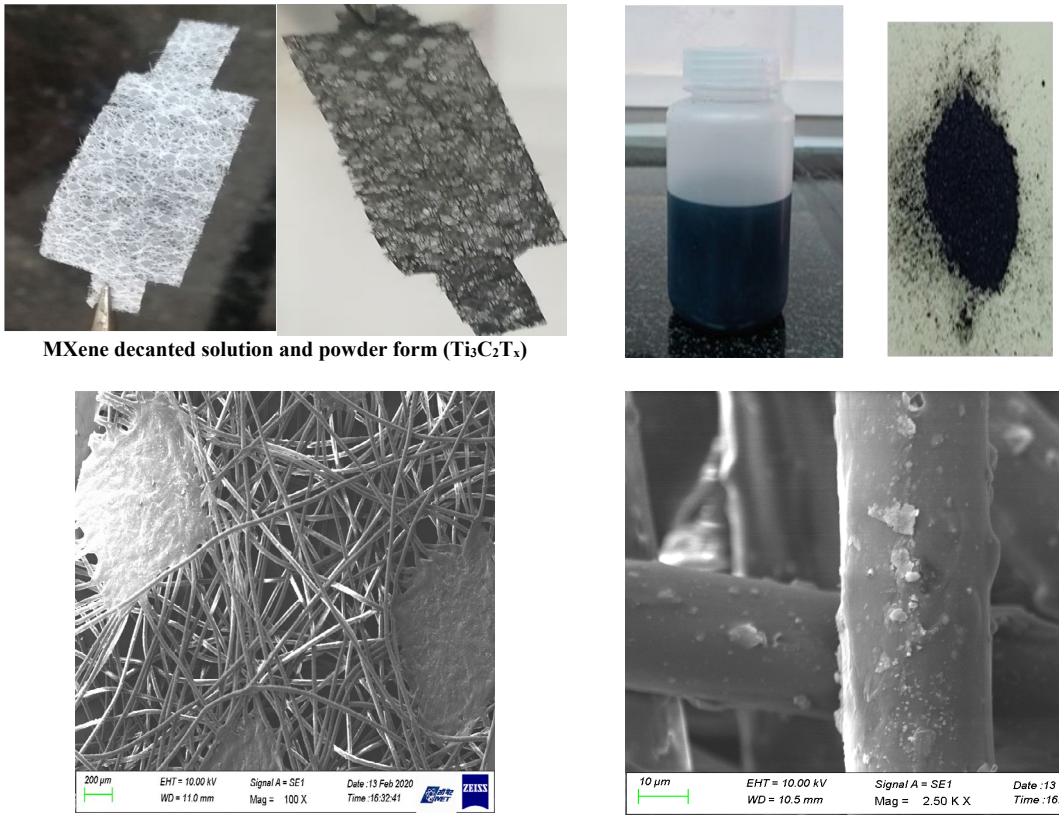

Fig. 4. FE-SEM images of coated and uncoated MXene non-woven paper materials.

From the Figure 5 it's further noticed that Micrographs of $Ti_3C_2T_X$ coated non-woven cotton paper show highly closely packed deposit of $Ti_3C_2T_x$ which is responsible for the observed conductivity. This is in consistent with the XRD results. From the above results form figure 5, confirms indirectly the optimized coating for improved amount of titanium deposition on paper cloth materials are [C- 19.2, F- 4.2, Ti- 47.2(p2) and C- 31.7, F- 4.2, Ti-41.4 (p3)]. Figure 6 shows the Raw material morphology and EDS analysis of $Ti_3C_2T_X$ after the coating process to confirm the elemental content value obtained from higher magnification studies. The samples pelled of from the coated and analyzed further variation in elemental content after the experimental sensor study on above prepared MXene paper coated substrate [15,20-23]. Figure 6 revealed that the from P0-P3 are in the magnification scale of 5 um, and P4 recorded at 2 um scale. P4 shows the separate particles of aggregation obtained fatter aluminum removed from the precursor powder by etching process. We prepared very pure $Ti_3C_2T_X$ without any aluminum content in the final powder of the materials. Titanium atomic percentage is gradually increased from P0-P4 with improved morphological changes and uniform square/spherical particle morphology observed in the SEM image of P4 (Figure 6).

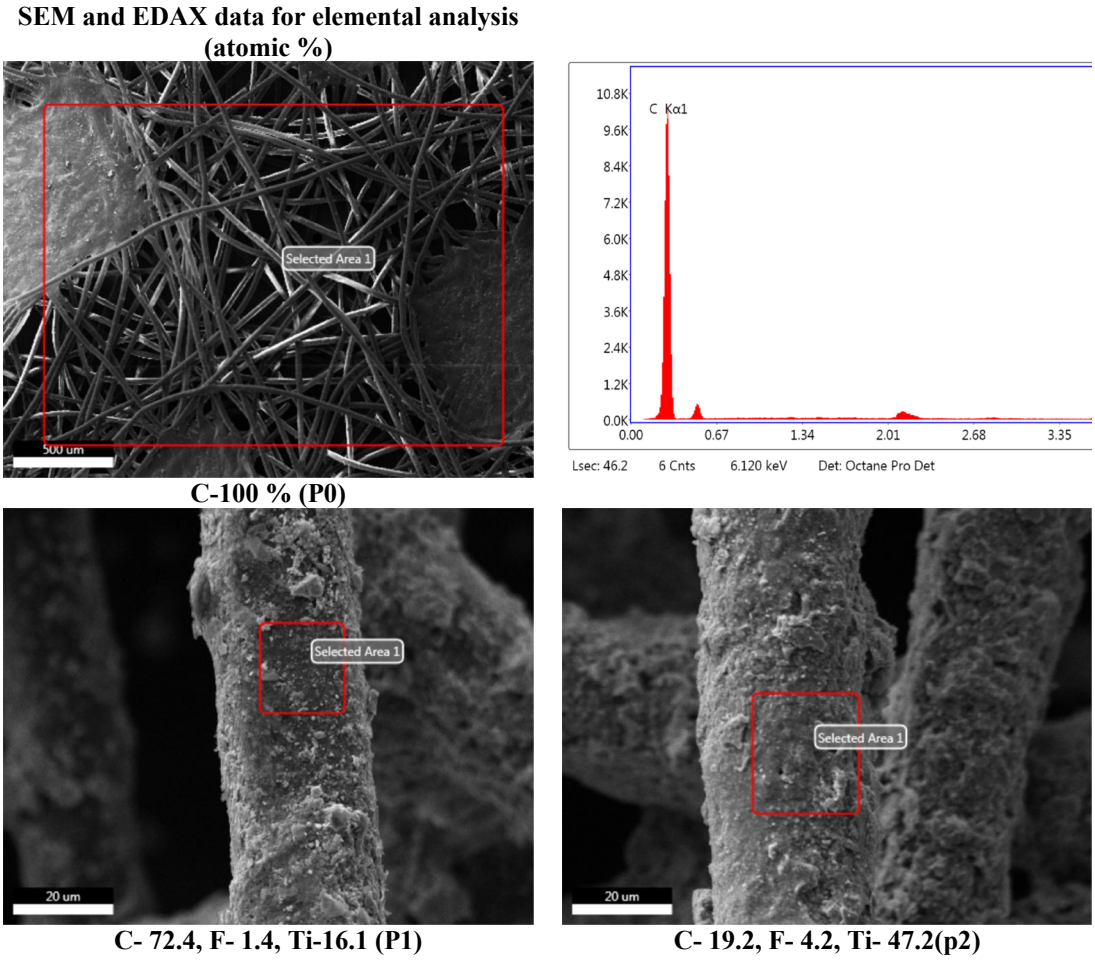

Fig. 5. SEM- EDS report of MXene $Ti_3C_2T_X$ coated non-woven cotton paper.

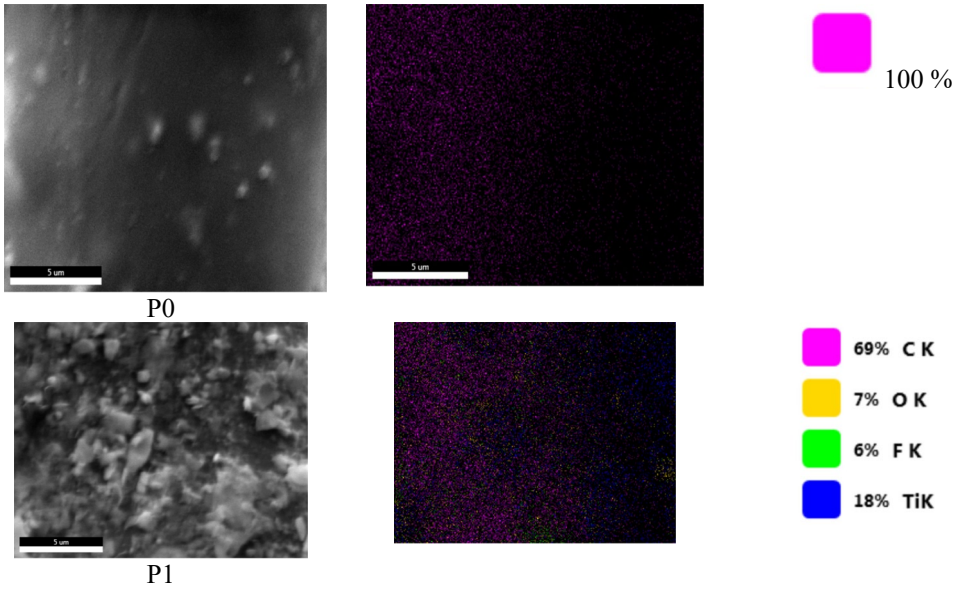

Fig. 6. SEM-EDS analysis of $Ti_3C_2T_x$ prepped in the present study via aluminum layer etching process.

The electrical properties of several coated substrates, including conductivity, resistivity, and bulk concentration, were examined. The conductivity of the $Ti_3C_2T_x$ drop cast on a glass substrate is 48.7S/cm. The very low conductivity of dip-coated textiles (0.02 S/cm) may be a result of the small amount of $Ti_3C_2T_x$ deposited and the same compared with other materials [23-29]. A large amount of $Ti_3C_2T_x$ can be deposited via drop casting on a glass substrate, resulting in excellent conductivity. However, the amount of $Ti_3C_2T_x$ deposited during dip coating may be reduced, resulting in a low conductivity. This may be enhanced by adjusting the coating conditions. The vacuum-filtered $Ti_3C_2T_x$ coated on membrane has an extremely low resistance of 44Ω. To further examine the $Ti_3C_2T_x$ -coated conducting surface, a 9V battery pack has been linked through coated surfaces to power an LED, as illustrated in the diagram below in Figure 7. It can be observed that the $Ti_3C_2T_x$ -coated on glass substrate emits lighter than membrane and cloth substrates. This is due to the high deposition and dense packing of $Ti_3C_2T_x$ deposited on a glass substrate via drop casting.

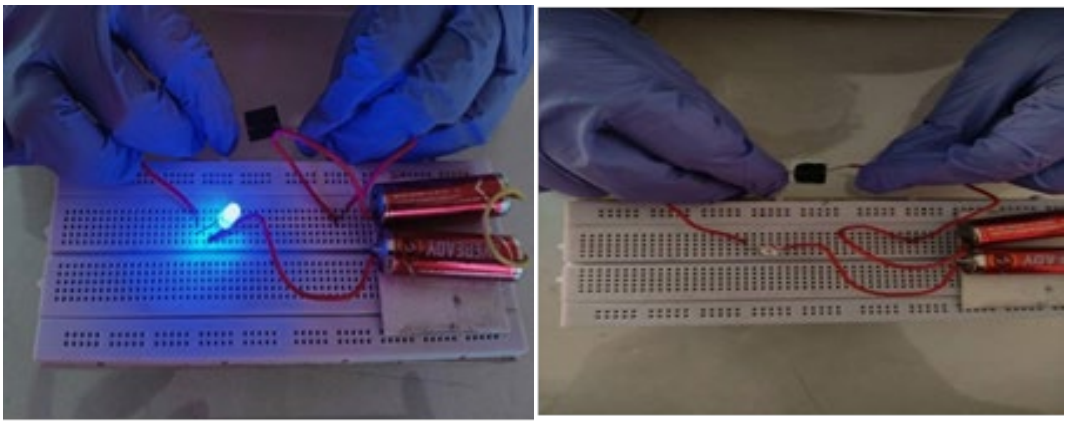

P1 *P2*

Fig. 7. Electrical property characteristics of $Ti_3C_2T_x$ coated on glass and non-woven paper cloth.

4.4. Application of 2D Coatings of MXene-in Water and its electromechanical analysis

MXene has a unique combination of mechanical, physical, and chemical properties. MXene flakes have surface terminations (Tx) like =–OH, O, and –F, rendering them hydrophilic and solution-processable. Additionally, MXene flakes are negatively charged, exhibit strong mechanical strength, and electrical conductivity, and have intriguing intercalation capabilities of ions and big organic molecules. These features permitted MXene to be utilized as a very advanced platform for the detection of phonations and substantial motions such as waking, jumping, running, and other human actions such as coughing, joint bending, etc. Figures 4 and 5 show morphological images of (a) $Ti_3C_2T_x$ coated membrane and (b and c) resistance measuring using fluke with different distances. $Ti_3C_2T_x$ coated membrane (0.5 X 3 cm) acted as a bending sensor. For a fine change of lengths, the resistance value quickly with a huge hike. Resistance value measured using fluke (“8846A, 6 ½ Digital precision multimeter”). Table 5.1 shows resistance value variation with resistance. Variations in frequency can be observed in relation to finger bending. When prototype sensor was affixed to finger, it continuously displayed variations in waveform as the finger bent. Consequently, the impact of finger bending may be deduced from the observed variations in oscilloscope's frequency waveform. The $Ti_3C_2T_x$ -coated membrane and paper cloth can be employed as a strain sensor prototype for sensing finger bending and body movement.

Table 1. Resistance of $Ti_3C_2T_x$coated membrane.

Length (cm)	Resistance measured (kΩ)						
	1	**2**	**3**	**4**	**5**	**6**	**7**
3	21.5627	25.5432	30.0103	57.0312	57.0090	60.1392	63.1161
2.5	20.4236	24.1459	29.9854	53.0021	54.7901	58.9160	61.7420
2	19.0492	22.4278	23.8414	49.5314	52.2391	55.7361	60.7612
1.5	18.3920	19.3981	21.4512	35.2586	37.6831	42.8319	57.1258
1	17.4312	19.0001	21.1385	32.4236	35.1459	39.9854	55.0021

5. Conclusions

In this work, the preparation and properties of $Ti_3C_2T_x$, a representative of a new family of 2D materials known as MXenes, was investigated. Particular attention was given to studying the effect of preparation conditions, properties and to understand its potential applications in the field electronics as well as photonics. From the preparation procedure it shows that the concentration of HCl, Ti_3AlC_2: LiF ratio and reaction time of synthesis play an important role in etching of Al to form $Ti_3C_2T_x$. Even though highly delaminated Ti_3C_2Tx could obtain by the in-situ HF etching method, there are still some challenges for obtaining uniform material. Developing moderate and safe synthesis routes with high yield and low cost is of necessity to realize the practical application of Ti_3C_2Tx. More efforts are needed to explore its properties and applications. In future, more investigations are expected to address these challenges to further promote application of MXene-based materials for electronics/ photonics applications in the field of energy and healthcare.

Acknowledgements

The authors express thankful and financial support by the Researchers Supporting Project Number (RSP-2024R354) King Saud University, Riyadh, Saudi Arabia.

References

[1] Zhang, S., Chhetry, A., Zahed, M. A., Sharma, S., Park, C., Yoon, S., Park, J. Y. (2022). npj Flexible Electronics, 6(1), 11; https://doi.org/10.1038/s41528-022-00140-4

[2] Yan, W., Fuh, H. R., Lv, Y., Chen, K. Q., Tsai, T. Y., Wu, Y. R., Wu, H. C. (2021). Nature communications, 12(1), 2018; https://doi.org/10.1038/s41467-021-22316-8

[3] Lee, K. S., & El-Sayed, M. A. (2006), The Journal of Physical Chemistry B, 110(39), 19220-19225; https://doi.org/10.1021/jp062536y

[4] Pei, Y., Zhang, X., Hui, Z., Zhou, J., Huang, X., Sun, G., Huang, W. (2021), ACS nano, 15(3), 3996-4017; https://doi.org/10.1021/acsnano.1c00248

[5] Yang, H., Li, J., Xiao, X., Wang, J., Li, Y., Li, K. & Chen, P. Y. (2022), Nature Communications, 13(1), 5311; https://doi.org/10.1038/s41467-022-33021-5

[6] Redondo, E., & Pumera, M. (2021), Electrochemistry Communications, 124, 106920; https://doi.org/10.1016/j.elecom.2021.106920

[7] Wang, Q., Han, N., Shen, Z., Li, X., Chen, Z., Cao, Y., Thakur, V. K. (2022), Nano Materials Science; https://doi.org/10.1016/j.nanoms.2022.07.003

[8] Babar, Z. U. D., Della Ventura, B., Velotta, R., & Iannotti, V. (2022), RSC advances, 12(30), 19590-19610; https://doi.org/10.1039/D2RA02985E

[9] Murugan, N., Jerome, R., Preethika, M., Sundaramurthy, A.,Sundramoorthy, A. K. (2021). Journal of Materials Science & Technology, 72, 122-131; https://doi.org/10.1016/j.jmst.2020.07.037

[10] Kang, R., Zhang, Z., Guo, L., Cui, J., Chen, Y., Hou, X., Yu, J. (2019), Scientific reports,

9(1), 9135; https://doi.org/10.1038/s41598-019-45664-4
[11] Zhao, H., Ding, J., Zhou, M., & Yu, H. (2021), ACS Applied Nano Materials, 4(3), 3075-3086; https://doi.org/10.1021/acsanm.1c00219
[12] Mehdi Aghaei, S., Aasi, A., & Panchapakesan, B. (2021), ACS omega, 6(4), 2450-2461; https://doi.org/10.1021/acsomega.0c05766
[13] Wang, S., Shao, H. Q., Liu, Y., Tang, C. Y., Zhao, X., Ke, K., Yang, W. (2021). Composites Science and Technology, 202, 108600; https://doi.org/10.1016/j.compscitech.2020.108600
[14] Yu L, Liu B, Wang Y, Yu F, Ma J., J Power Sources 2021;490:229250; https://doi.org/10.1016/j.jpowsour.2020.229250
[15] Song P, Liu B, Qiu H, Shi X, Cao D, Gu J. M, Compos Commun 2021;24; https://doi.org/10.1016/j.coco.2021.100653
[16] Li Q, Yin R, Zhang D, Liu H, Chen X, Zheng Y, et al., J Mater Chem A 2020;8:21131-41; https://doi.org/10.1039/D0TA07832H
[17] Yu L, Liu B, Wang Y, Yu F, Ma J., J Power Sources 2021;490:229250; https://doi.org/10.1016/j.jpowsour.2020.229250
[18] Song P, Liu B, Qiu H, Shi X, Cao D, Gu J. M., Compos Commun 2021;24. https://doi.org/10.1016/j.coco.2021.100653
[19] Li Q, Yin R, Zhang D, Liu H, Chen X, Zheng Y, et al., J Mater Chem A 2020;8:21131-41; https://doi.org/10.1039/D0TA07832H
[20] Kumar YR, Deshmukh K, Ali MMN, Rajabathar JR, Theerthagiri J, Pandey M, et al. Structure defects and electronic properties of MXenes. 2021; https://doi.org/10.1016/B978-0-12-823361-0.00005-8
[21]Wang Y, Peng H-K, Li T-T, Shiu B-C, Ren H-T, Zhang X, et al., Chem Eng J 2021;412; https://doi.org/10.1016/j.cej.2021.128681
[22] Zamhuri A, Lim GP, Ma NL, Tee KS, Soon CF. Biomed Eng Online 2021;20; https://doi.org/10.1186/s12938-021-00873-9
[23] Liu H, Li Q, Bu Y, Zhang N, Wang C, Pan C, et al., Nano Energy 2019;66:104143; https://doi.org/10.1016/j.nanoen.2019.104143
[24] Jothi Ramalingam R, Arunachalam P, Amer MS, AlOthman ZA, Alanazi AG, AL-Anazy MM, et al., Intermetallics 2021;131; https://doi.org/10.1016/j.intermet.2021.107101
[25] Song P, Liu B, Qiu H, Shi X, Cao D, Gu J., Compos Commun 2021;24; https://doi.org/10.1016/j.coco.2021.100653
[26] Hasan MM, Hossain MM, Chowdhury HK., J Mater Chem A 2021;9:3231-69; https://doi.org/10.1039/D0TA11103A
[27] S NK, R JR, Karnan M, N P K., Chem Eng Process - Process Intensif 2023;185; https://doi.org/10.1016/j.cep.2023.109305
[28]. Gagan Kumar SK, Santhosh AS, Sumana S, Trishul AM, Sandeep S, Karthik CS, et al., Surfaces and Interfaces 2023;37; https://doi.org/10.1016/j.surfin.2023.102744
[29] Rajabathar JR, Al-Lohedan HA, Arokiyaraj S, Issa ZA, Dash CS, Murugesan S, et al., Coatings 2021;11:1-20; https://doi.org/10.3390/coatings11101150